Journal of Electroceramics, 13, 543–548, 2004

Electrical Properties of Bismuth Titanate Based Ceramics with Secondary Phases

M. VILLEGAS, T. JARDIEL, A.C. CABALLERO & J.F. FERNÁNDEZ
Electroceramics Department, Instituto de Cerámica y Vidrio – CSIC, 28049 Cantoblanco, Madrid, Spain

Submitted February 18, 2003; Revised October 30, 2003; Accepted November 6, 2003

Abstract. $Bi_4Ti_3O_{12}$ (BIT) based ceramics were prepared by hydroxide coprecipitation method and subsequent treatment at 650°C for 1 h. Calcined BIT was doped with different amounts of WO_3 by surface doping using $W(C_2H_5O)_6$. The amount of dopant modified the sintering behaviour of BIT-based ceramics through a liquid-phase assisted sintering mechanism in the case of low dopant concentration and Zenner effect when high concentration of dopant was used. Consequently, the microstructure and the electrical properties were strongly dependent on the dopant concentration. Doped BIT-based ceramics showed a microstructure composed of very small platelet-like grains and the electrical conductivity was markedly decreased. The high electrical resistivity makes possible the polarization of doped ceramics and relatively good piezoelectric parameters were measured.

Keywords: bismuth titanate, microstructure, piezoelectric properties

Introduction

Bismuth titanate $Bi_4Ti_3O_{12}$, BIT, is a high temperature ferroelectric ceramic (Tc = 675°C) [1] with useful properties for optical memory, piezoelectric and electro-optic devices [2, 3].

BIT belongs to the Aurivillius family of bismuth-based layered perovskites and consists of layers of perovskite-like units $(Bi_2Ti_3O_{10})^{2-}$ interleaved between bismuth oxide based layers $(Bi_2O_2)^{2+}$ [4]. The crystal structure promotes a plate-like morphology with the $(Bi_2O_2)^{2+}$ layers in the *ab* plane due to the large anisotropy in the surface energy.

One of the major difficulties for the use of BIT ceramics in piezoelectric applications is their high electrical conductivity, which interferes with the poling process. In addition to this, the high anisotropy of electrical conductivity [5] makes the microstructure play a critical role in the electrical properties, being the electrical conductivity dependent on the aspect ratio (length/thickness) of the platelet-like grains [6]. In this sense, the dependence of the electrical conductivity on microstructure makes ceramic processing a critical step in achieving BIT ceramics with practical use [7].

Donor doping, Nb(V), W(VI), significantly decreases the conductivity in BIT-based ceramics [6–9]. This effect has been attributed to a reduction of space charge build up by the compensation of Bi vacancies accompanied by oxygen vacancies [10].

The objective of this work was to study the influence of different amounts of W(VI) as donor dopant on the sintering, appearance of secondary phases, microstructure and the influence of these parameters on the electrical properties of BIT in order to improve the piezoelectric properties.

Experimental Procedure

Undoped BIT ceramics were obtained by hydroxide coprecipitation method using $BiNO_3{\cdot}5H_2O$ (Riedel-deHaën, 98%) and $Ti(C_4H_9O)_4{\cdot}C_4H_9OH$ (Alfa Aesar, 99%) as Bi_2O_3 and TiO_2 precursors. Experimental details were reported elsewhere [11]. The coprecipitated powders were air-calcined at 650°C/1 h. Doping was done by particle surface coating using $W(C_2H_5O)_6$ (Alfa Aesar, 99.8%) as a source of W(VI) [12]. Ceramic powders with a general formula $Bi_4Ti_3W_xO_{12}$ with $x = 0$, 0.08 and 0.15 were obtained. Undoped and doped BIT ($x = 0.08$ BITW8, $x = 0.15$ BITW15) were uniaxially pressed into disks and air-sintered between 850–1150°C (for undoped BIT) and 950–1150°C (for doped BIT) with a soaking time of 2 h.

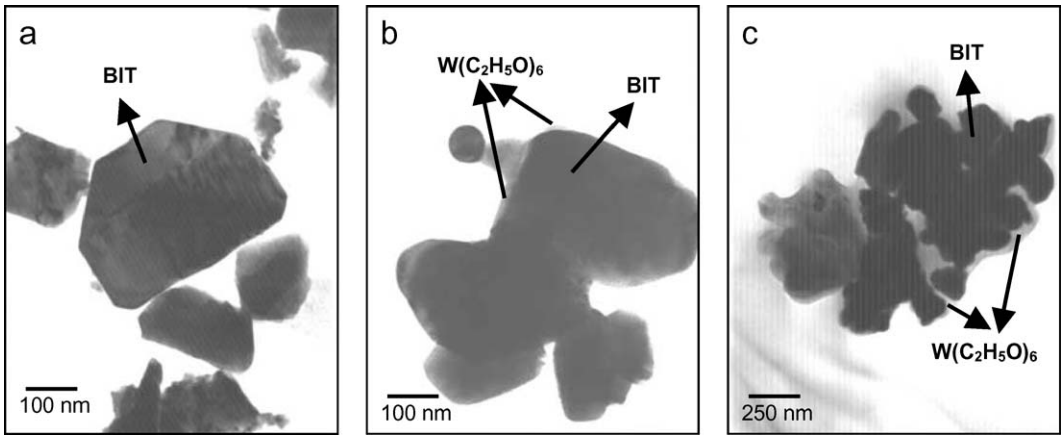

Fig. 1. TEM micrographs of BIT-based ceramic powders. (a) BIT, (b) BITW8, and (c) BITW15.

Ceramic powders were characterized by means of TEM (Hitachi 7100). After sintering, the apparent density of samples was measured by the Archimedes method in water and the weight losses were determined by weighing the samples before and after sintering. The phase composition and lattice parameters were determined by means of XRD (Siemens D5000) using Si as internal standard. The microstructure was studied by SEM (Carl Zeiss DSM950 equipped with EDS) on polished and thermally etched surfaces. Aspect ratio of platelet-like grains was measured by means of an Image Analyzer on at least 300 grains. Electrical characterization was performed on Ag-electroded disks using an impedance analyzer (HP 4192A) in the temperature range of 25–740°C. Piezoelectric charge constant d_{33} was measured on samples poled with an electric field of 60 kV/cm at 180°C for 1 h using a d_{33} Berlincourt piezo-meter.

Experimental Results

Figure 1 shows the undoped and doped BIT ceramic powders characterized by TEM. Undoped BIT was composed of platelet-like particles of about 300–500 nm that did not show appreciable agglomeration. BITW8 particles were slightly more rounded and in some of them the surface coating with W(VI) can be appreciated. However, the coating is preferentially located between the particles and thus the agglomeration is promoted by the dopant precursor. In the case of BITW15 islands of particles appear completely surrounded by the W(VI) precursor and no individual particles were observed, neither coated nor uncoated.

During sintering, BITW8 reached the highest density, 98% of theoretical density (d_{th}), at 1050°C, whereas the maximum density of BIT and BITW15 was similar (95% d_{th}) at 900°C for BIT and 1100°C for BITW15. Weight losses (<0.35%) increased with temperature in all cases due to Bi_2O_3 evaporation, being slightly higher for BITW8. Table 1 resume density values of sintered ceramics.

Figure 2(a) shows the XRD characterization of samples sintered at 1150°C. In BITW15 pattern the presence of a secondary phase $Bi_6Ti_3WO_{18}$ is clearly seen. Another secondary phase, $Bi_2Ti_2O_7$ is present in all samples at this temperature. In Fig. 2(b) the microstructure of BITW15-1150°C is depicted, showing the presence of secondary phases with both different morphology (bipyramidal grains) and size from those of BIT. Qualitative EDS analysis of bipyramidal secondary phase and platelets is also shown.

c lattice parameter for samples with an aspect ratio (length/thickness) $l/t = 3$ (BIT sintered at 900°C and

Table 1. Theoretical density (%) of sintered samples.

Sintering T (°C)	BIT	BITW8	BITW15
850	91.6 ± 0.6	–	–
900	95.1 ± 0.5	–	–
950	94.0 ± 0.5	80.3 ± 0.6	79.8 ± 0.6
1000	93.6 ± 0.5	93.6 ± 0.5	83.7 ± 0.6
1050	92.6 ± 0.6	97.6 ± 0.5	90.8 ± 0.6
1100	90.8 ± 0.6	95.4 ± 0.5	94.8 ± 0.5
1150	88.0 ± 0.6	87.0 ± 0.6	88.7 ± 0.6

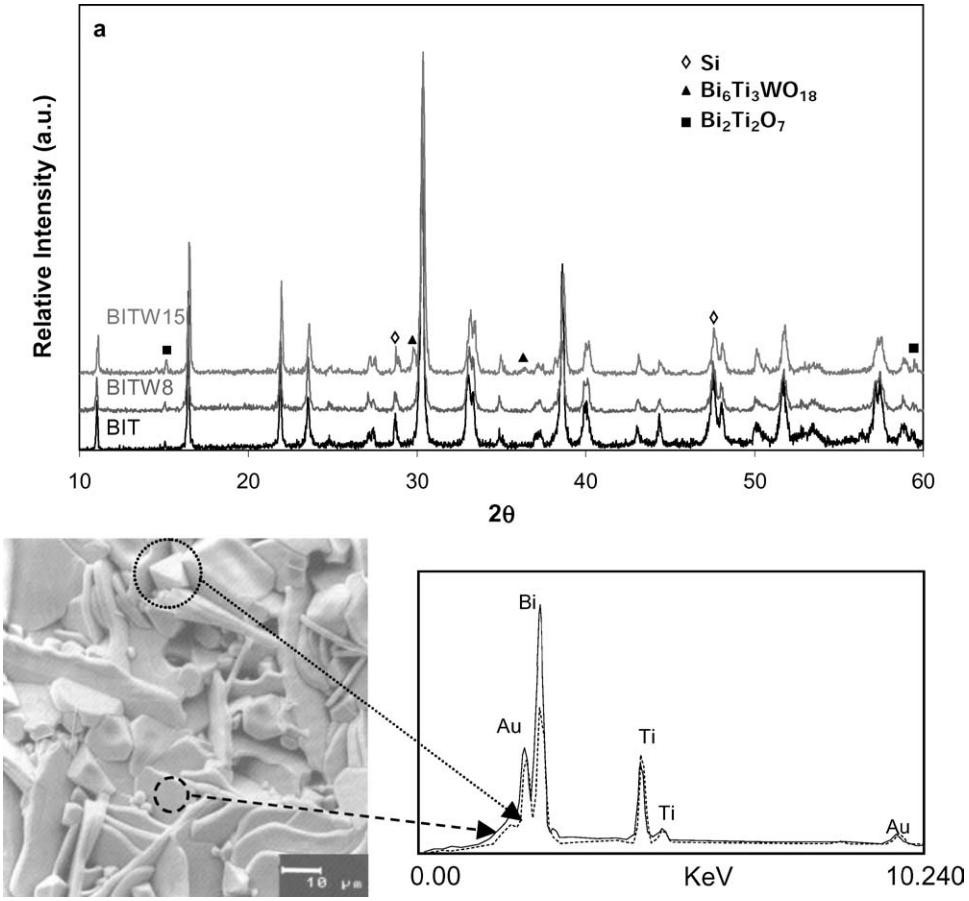

Fig. 2. (a) XRD pattern of BIT-based ceramics sintered at 1150°C and (b) SEM micrograph of BITW15 (1150°C).

BITW8 at 1100°C and BITW15 at 1050°C) increased by dopant content in a higher extent when $x = 0.08$ than for $x = 0.15$. a and b lattice parameters increased very slightly by doping. Table 2 resume the lattice parameters for the different BIT-based ceramics.

Figure 3 shows the microstructure of BIT-based ceramics sintered at 1050°C. Doping decreased average grain size, from platelets of about 15 μm in length for BIT to platelets of 2–3 μm for W-doped ceramics. Another distinct feature is the change in shape for BITW8 which presented platelets much more rounded than BIT and BITW15.

Table 2. Lattice parameters (samples with $l/t = 3$).

Sample	a (Å)	b (Å)	c (Å)
BIT-900°C	5.445 ± 0.001	5.407 ± 0.001	32.808 ± 0.001
BITW8-1100°C	5.444 ± 0.001	5.413 ± 0.001	32.858 ± 0.001
BITW15-1050°C	5.437 ± 0.001	5.412 ± 0.001	32.823 ± 0.001

In Fig. 4 the ln σ at 540°C for BIT-based ceramics with $l/t = 3$ is shown. Electrical conductivity decrease by donor doping is clearly observed for $x = 0.08$. However, when dopant concentration increases there is not a further reduction of electrical conductivity. The reduction of electrical conductivity allowed to pole W-doped samples. Table 3 resume the piezoelectric charge constant d_{33} measured for BITW8 and BITW15.

Table 3. Piezoelectric charge constant d_{33} for W-doped BIT ceramics.

Sample	Sintering temperature (°C)	d_{33} (pC/N)
BITW8	1050°C	15 ± 2
	1100°C	17 ± 2
BITW15	1050°C	18 ± 2
	1100°C	22 ± 2

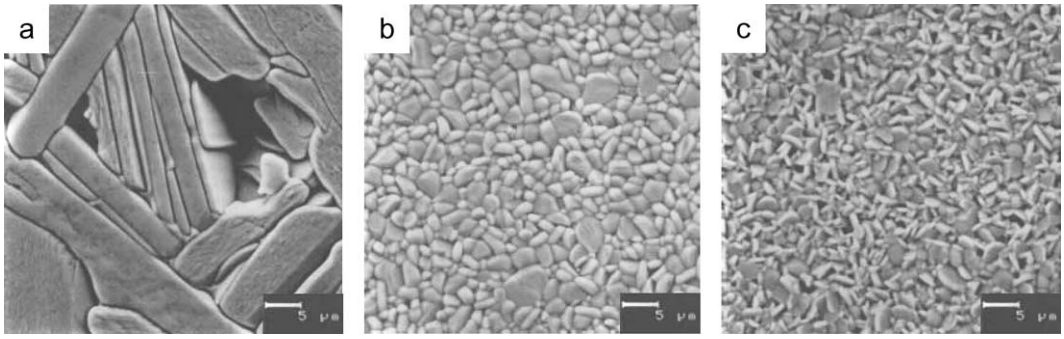

Fig. 3. SEM micrographs of samples sintered at 1050°C. (a) BIT, (b) BITW8 and (c) BITW15.

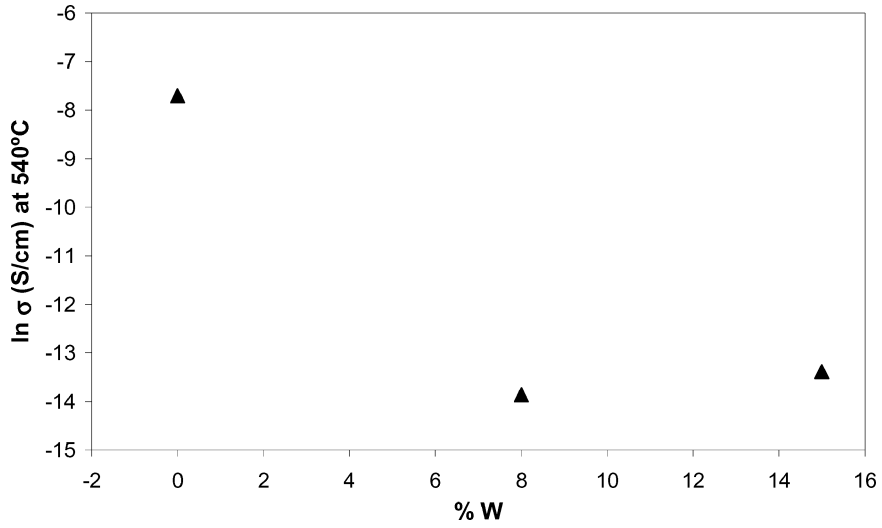

Fig. 4. ln σ at 540°C as a function of dopant concentration for samples with $l/t = 3$ (BIT-900°C, BITW8-1100°C and BITW15-1050°C).

Discussion

Sintering behaviour of BIT-based ceramics was modified by the amount of dopant. This change, due to the presence of WO_3 surrounding BIT particles, points to a densification process controlled by a solute drag mechanism. W^{6+} seems to be rate controlling grain boundary diffusion [7].

The increase of weight losses with temperature is related to the increase of Bi_2O_3 losses, by the following reaction:

$$2Bi_4Ti_3O_{12} \rightarrow Bi_2O_3(\uparrow) + 3Bi_2Ti_2O_7$$

$Bi_2Ti_2O_7$ is present in sintered samples, as it is shown in Fig. 2(a).

On the other hand, there is an increase of weight losses when dopant is present, indicating that the presence of WO_3 induces loss of Bi_2O_3 from BIT. This is due to the charge compensation mechanism, which generates Bi vacancies.

$$Bi_4Ti_3O_{12} + WO_3 \rightarrow Bi_{4-x}(V'''_{Bi})_xTi_3W_xO_{12} + x/2Bi_2O_3 + 3x/4O_2$$

However, weight losses up to 1100°C for BITW15 were somewhat lower than in BITW8 ceramics. Taking into account the previous charge compensation mechanism, if W(VI) completely incorporates BIT lattice in BITW15, weight losses should be higher. The appearance of the secondary phase $Bi_6Ti_3WO_{18}$ (see Fig. 2(b)) indicates that part of the WO_3 available is not

incorporating BIT lattice but reacting with the Bi_2O_3 evaporated compensating in part the weight losses, through the following reaction:

$$Bi_4Ti_3O_{12} + WO_3 + Bi_2O_3 \rightarrow Bi_6Ti_3WO_{18}$$

The presence of this secondary phase modifies the sintering behaviour of BITW15 ceramics through a pinning effect exerted by the grains of $Bi_6Ti_3WO_{18}$ (see Fig. 2(b)), probably being this phase the smallest grains. Their composition could not be determined by EDS due to their small size and the very low amount of tungsten. Bipyramidal grains should be $Bi_2Ti_2O_7$, taking into account its pyrochlore-based structure [13, 14]. EDS qualitative analysis of these bipyramidal grains showed a lower Bi/Ti ratio than in platelets, as corresponds to $Bi_2Ti_2O_7$ compared to $Bi_4Ti_3O_{12}$.

The smaller variation of c lattice parameter in BITW15 than in BITW8 corroborates that part of the WO_3 available is consumed in the formation $Bi_6Ti_3WO_{18}$ secondary phase so not all the W(VI) is diffusing into BIT lattice. On the contrary, this fact indicates the almost complete incorporation of W(VI) in BiTW8. The increase of c lattice parameter is due to a reduction of the interaction between perovskite-like and $(Bi_2O_2)^{2+}$ layers as a consequence of a higher interaction between W^{6+} in B positions of the perovskite and the oxygens in octahedral positions because of the higher electronegativity of W^{6+} as compared with Ti^{4+} ($W = 2.06$ Pauling scale; Ti = 1.54 Pauling scale). The shortening of W-O bonds in perovskite-like layer enlarges the bonding between Bi in the $(Bi_2O_2)^{2+}$ layer and the apical oxygen of the perovskite thus producing the increase of c lattice parameter.

Microstructure of BIT-based ceramics also reflected the different incorporation of W(VI) into BIT grains. For BITW8 there is a strong decrease of average grain size with respect to undoped BIT. The presence of a layer of tungsten precursor surrounding BIT particles (see Fig. 1) controls grain growth in BITW8 through the solute drag mechanism. As it have been shown, the incorporation of WO_3 into BIT lattice enhances the loss of Bi_2O_3 through charge compensation, this could be the reason of the presence of rounded platelets in BITW8, due to the presence of a transitory liquid phase during sintering. There is also a strong decrease of average grain size in BITW15, but the reason for this decrease seems to be different to that of BITW8. In this case, platelets are not rounded being their shape similar to those of undoped BIT but smaller. The formation of the secondary phase $Bi_6Ti_3WO_{18}$ in BITW15 ceramics consumed the evaporated Bi_2O_3 so no transitory liquid phase is formed. In addition, the presence of small grains of $Bi_6Ti_3WO_{18}$ that exerted a pinning on grain boundaries should be the reason of the grain growth control.

Electrical conductivity was reduced in about 3 orders of magnitude when $x = 0.08$ for samples in which the dependence of the electrical conductivity with the aspect ratio of the platelets was considered (all samples $l/t \approx 3$). In this manner, the effect of donor doping is shown. However, there is not a further reduction in electrical conductivity when $x = 0.15$, due to the incorporation of only a part of the dopant available, as it was discussed above. The reduction of electrical conductivity by donor doping should be produced by the reduction of positively charged carriers (oxygen vacancies or holes) by the generation of negatively charged carriers (bismuth vacancies or electrons) [10, 15, 16]. The nature of charge carriers in BIT ceramics is not still clear.

The decrease in electrical conductivity in BITW8 and BITW15 allowed to pole these ceramics to overcome the high coercive field of BIT-based ceramics. Piezoelectric charge constants (Table 3) are similar for both types of doped ceramics, although they are a slightly higher when $x = 0.15$. The reason for such behaviour is still not known by the authors, however piezoelectric parameters are very promising.

Conclusions

The effect of different amounts of donor dopant W(VI) on the sintering, microstructure and electrical properties of $Bi_4Ti_3W_xO_{12}$ ($x = 0.08$, 0.15) ceramics was studied. The sintering mechanism was modified by the amount of dopant and when $x = 0.08$ the solute drag mechanism seemed to be controlling the densification. On the contrary, when $x = 0.15$ the mechanism seems to be a pinning of grain boundaries exerted by the presence of $Bi_6Ti_3WO_{18}$ secondary phase. This was in agreement with the microstructure development. As it was observed the addition of tungsten strongly decreased average grain size, but the shape of platelets was different for BITW8 and BITW15, being more rounded in the first case indicating the possible presence of a transitory Bi_2O_3-rich liquid phase induced by the charge compensation mechanism produced by the incorporation of W(VI) to the BIT lattice. In the

case of BITW15 the shape of the platelets was similar to that of undoped BIT indicating the absence of the Bi_2O_3-rich liquid phase because the evaporated Bi_2O_3 was consumed in the formation of $Bi_6Ti_3WO_{18}$ secondary phase. Lattice parameter variation corroborates this assumption. Electrical conductivity was reduced in about 3 orders of magnitude in doped samples. The effect of donor doping was evident if it is taken into account that the effect of the aspect ratio of the platelets was suppressed. The reduction in electrical conductivity allowed to pole doped ceramics and very promising piezoelectric charge constants d_{33} were measured.

Acknowledgments

This research was supported by the Spanish Comisión Interministerial de Ciencia y Tecnología (CICYT) under Project MAT2001-1682-C02-01.

References

1. E.C. Subbarao, *J. Phys. Chem. Solids*, **23**, 665 (1962).
2. T. Takenaka and K. Sakata, *J. Appl. Phys.*, **55**, 1092 (1984).
3. J.F. Scott and C.A. Araujo, *Science*, **246**, 1400 (1989).
4. B. Aurivillius, *Ark. Kemi*., **1**, 499 (1949).
5. A. Fouskova and L.E. Cross, *J. Appl. Phys.*, **41**, 2834 (1970).
6. M. Villegas, A.C. Caballero, C. Moure, P. Durán, and J.F. Fernández, *J. Am. Ceram. Soc.*, **82**, 2411 (1999).
7. M. Villegas, A.C. Caballero, and J.F. Fernández, *Ferroelectrics*, **267**, 165 (2002).
8. S.S. Lopatin, T.G. Lupeiko, T.L. Vasil'tsova, N.I. Basenko, and I.M. Berlizev, *Inorg. Mater.*, (Engl. Transl.) **24**, 1328 (1988).
9. H.S. Shulman, M. Testorf, D. Damjanovic, and N. Setter, *J. Am. Ceram. Soc.*, **79**, 3124 (1996).
10. J.S. Kim, S.S. Kim, J.K. Kim, and T.K. Song, *Jpn. J. Appl. Phys.*, **41**, 6451 (2002).
11. M. Villegas, C. Moure, J.F. Fernández, and P. Durán, *Ceram. Int.*, **22**, 15 (1996).
12. M. Villegas, T. Jardiel, and G. Farías, *J. Eur. Ceram. Soc.* **24**, 1025 (2004).
13. I. Radosavljevic, J.S.O. Evans, and A.W. Sleight, *J. Solid State Chem.*, **136**, 63 (1998).
14. S.P. Yordanov, I. Ivanov, and P. Carapanov, *J. Phys. D: Appl. Phys.*, **31**, 800 (1998).
15. A.Q. Jiang, G.H. Li, and L.D. Zhang, *J. Appl. Phys.*, **83**, 4878 (1998).
16. C. Voisard, D. Damjanovic, and N. Setter, *J. Europ. Ceram. Soc.*, **19**, 1251 (1999).